Applied Surface Science 254 (2008) 5564–5568

Contents lists available at ScienceDirect

Applied Surface Science

journal homepage: www.elsevier.com/locate/apsusc

Comparison and semiconductor properties of nitrogen doped carbon thin films grown by different techniques

F. Alibart [a], O. Durand Drouhin [a], M. Benlahsen [a,*], S. Muhl [b], S. Elizabeth Rodil [b], E. Camps [c], L. Escobar-Alarcon [c]

[a] Laboratoire e Physique de la Matière Condensée, 33 rue Saint Leu, 80000 Amiens, France
[b] Instituo de Investigationes en Materials, Universidad National Autonomia de Mexico, Mexico, D.F. 04510, Mexico
[c] Instituo National de Investigationes Nucleares, Apdo. Postal 18-1027, Mexico, D.F. 11801, Mexico

ARTICLE INFO

Article history:
Received 16 October 2007
Received in revised form 28 February 2008
Accepted 29 February 2008
Available online 6 March 2008

PACS:
78.40.Fy
81.05.Hd
81.15.Fg

Keywords:
Carbon nitride
DC sputtering
Radio frequency magnetron sputtering
Pulsed laser deposition

ABSTRACT

Amorphous carbon nitride (a-CN_x) thin films have been synthesised by three different deposition techniques in an Ar/N_2 gas mixture and have been deposited by varying the percentage of nitrogen gas in the mixture (i.e. the $N_2/Ar + N_2$ ratio) from 0 to 10%. The variation of the electrical conductivity and the gap values of the deposited films versus the $N_2/Ar + N_2$ ratio were investigated in relation with their local microstructure. Film composition was analysed using Raman spectroscopy and optical transmission experiments. The observed variation of electrical conductivity and optical properties are attributed to the changes in the atomic bonding structures, which were induced by N incorporation, increasing both the sp^2 carbon content and their relative disorder. The low N content samples seem to be an interesting material to produce films with interesting properties for optoelectronic applications considering the facility to control the gas composition as a key parameter.

1. Introduction

Amorphous carbon nitride thin films (a-CN_x) have been intensively studied during the last twenty years due to their promising mechanical properties predicted from the theoretical studies of the β-C_3N_4 crystalline structures [1]. The high hardness and strong resistance to wear, comparable to those of diamond, would make this material valuable and much wanted material for industrial applications such as the coating of mechanical parts. Various techniques have been used for the preparation of the carbon nitride films under a wide range of deposition parameters [2–5]. Although, most of the synthesised materials have nitrogen content lower than the stoichiometric proportion for the C_3N_4 (57 at.%), the new amorphous a-CN_x phases are of both scientific and practical interest [2–5], in particular in the field of optoelectronic devices, such as, gate insulator for OTFT, electron injection layer in OLEDs, or active layer in TFTs but the industrial utilisation of such films is still not of actuality [6–10].

From the numerous studies conducted on the a-CN_x, it has been clearly shown that the method of nitrogen incorporation (i.e. deposition conditions and system) determines both the nitrogen content and the prevalent C–N bonding configuration (sp^1, sp^2 and sp^3) in the deposited film, and therefore their physical properties. It has been reported that N atoms and CN radicals are the main precursors for the deposition of amorphous a-CN_x films in intense nitrogen discharges [5,11–12].

According to the literature, the properties of amorphous carbon (a-C) films are governed mainly by the nitrogen content, the substrate temperature and the energy of carbon species during deposition [2,11]. The aim of this study was to investigate the effect of nitrogen incorporation on the electrical and optical properties of the films comparing three different deposition techniques. The used techniques were Direct Current (DC) magnetron sputtering, DC pulsed magnetron sputtering and RF magnetron sputtering. A common feature of all these techniques is that the carbon species arriving at the substrate have a definite energy (or energy range) which can be varied and the deposited

* Corresponding author.
E-mail address: mohamed.benlahsen@sc.u-picardie.fr (M. Benlahsen).

0169-4332/$ – see front matter © 2008 Elsevier B.V. All rights reserved.
doi:10.1016/j.apsusc.2008.02.108

carbon films can exhibit a large variety of properties ranging from diamond-like to graphite-like. For instance, the DC and the RF sputtering techniques give amorphous carbon (a-C) films with more graphitic properties [2,5,13], whereas the use of pulsing DC is based on the encouraging results about the plasma parameters, which suggest larger ion flux densities and energies which might promote diamond-like properties [14]. Thus, the variety of a-CN_x film properties stems from variations in deposition conditions and the specific deposition scheme. It is clear that in order to obtain films with prescribed properties it is necessary to study how either property depends on deposition parameters within a chosen deposition technique. The present work focuses on the role of the nitrogen incorporation in the electrical resistivity and micro-structure of a-CN_x films. The characterisation methods include Raman scattering, optical spectroscopy and resistivity measurements.

2. Experimental details

The a-CN_x thin films have been deposited on corning glass and undoped Si (1 0 0) substrates at room temperature after a cleaning process of ultrasonic bathes in acetone and propanol. For all the sputtering techniques, the composition of the gas mixture (Ar/N_2) has been varied keeping the total pressure and power constant (about 1.2 Pa). Films with different nitrogen concentrations were deposited by varying the percentage of nitrogen gas in the mixture from 0 to 10% for the time deposition about 10 min at the substrate temperature close to 50 °C. Details of the deposition conditions and references are summarising in Table 1. The thicknesses of the films have been measured using a Dektak 3st profilometer.

The optical gap was determined by optical transmission measurements, in the 300–3000 nm range using a Varian *Cary 5* spectrometer in reflection and transmission mode. The analysis of the spectra has been carried out using a fitting analysis software. The model used to obtain the optical properties is based on the amorphous semiconductor band structure of Mott and Davis [17] providing the refractive index and the absorption coefficient in the UV–Vis–IR range. Raman spectra were performed at room temperature using a laser wavelength of 1064 nm of an Argon ion laser. The electrical measurements have been carried on a Keithley 6517A multimeter on glass substrates at room temperature. 60 nm thick Pt electrodes have been sputtered on a circular configuration to avoid any leakage currents. The electrical contacts have been verified to be ohmic, i.e. I(V) measurements, at the voltage value of conductivity measurement for each sample.

3. Results

Fig. 1 presents typical Raman spectrum of the a-CN_x films in the wave-number region of 900–2000 cm^{-1} deposited by the studied different techniques at given nitrogen fraction in the plasma (i.e. the $N_2/Ar + N_2$ ratio) about 2%. Raman spectra exhibit usually two main peaks centred approximately at 1550 cm^{-1}, corresponding to the G peak and at 1350 cm^{-1}, corresponding to the D peak. The G peak is due to in-plane bond stretching vibrations. This mode is a single resonance and can be present in aromatic rings as well as in olefinic chains. The D "disorder" mode is a double resonance and is

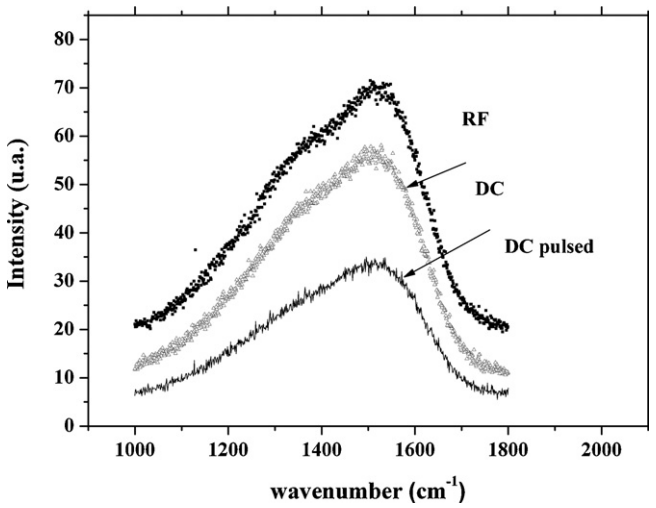

Fig. 1. Typical Raman spectra obtained at room temperature for samples deposited by different techniques. The excitation wavelength is of 1064 nm of an Argon ion laser. The laser power was limited to 50 mW in order to prevent any material heating and damage.

associated with breathing vibrations of aromatic rings. It can be present only in ring structures. The D peak is not present in the single crystalline graphite spectra or in completely amorphous carbon films [18–22]. The position, the integrated intensity ratio (I_D/I_G) of the D and G peaks and the full width at half maximum (ΔD and ΔG, respectively), can be used as an indicator for carbon bond arrangements. We have performed a computed deconvolution of the experimental Raman spectra in order to increase the accuracy of the estimation of these parameters. All these spectra were analysed by fitting with a BWF (Breit–Wigner–Fano) curve with a Lorentzian curve at the G and D positions with background correction.

We represent on Figs. 2 and 3 the variation of the I_D/I_G ratio and the G peak position versus the $N_2/Ar + N_2$ ratio. In the same trend as the previous results, both the I_D/I_G ratio and the G peak position increase for an increase of the $N_2/Ar + N_2$ ratio from 0 to 2–3%. The more important variations of the I_D/I_G ratio were seen for the DC and pulsed DC techniques where the values increased from 1 to 2.2 and 0.8 to 1.8, respectively. The RF samples showed only o slight increment from 1.2 to 1.6. Thus, an increase in I_D/I_G ratio is ascribed to an increase in the number and/or in the size of sp^2 clusters [21]. In the range of the studied N content, the position of the G peak shifts for the high values for all the techniques. Indeed, the RF samples present the larger value and vary with increasing N content from 1525 to 1550 cm^{-1}, while the DC and pulsed DC samples show an increase of G peak position from 1515 to 1545 cm^{-1}. This shows that the sp^2 sites have become ordered in a more aromatic fashion with increasing N contents. The saturation of the G band position at 1550 cm^{-1} (for RF samples) 1545 cm^{-1} (for DC samples) reflects the maximum possible Raman shift for C atoms bonded in sp^2 rings (noting that higher Raman shifts are possible for sp^2 C atoms found in chains, with shorter bond lengths), while for pulsed DC samples the saturation of the G band position at 1520 cm^{-1} reflects the more clustering character of these samples [18].

Table 1
Deposition conditions for the studied amorphous carbon nitride, which were grown for time deposition (t_{depos}) about 10 min

Technique	Pressure (Pa)	Power (W)	Gas composition	Frequency (Hz)	Deposition rate (nm/min) t_{depos} = 10 min	Reference
RF sputtering	1	200	$Ar + N_2$	13,56.E9	From 8 to 15	[5,27]
DC sputtering	1.3	200	$Ar + N_2$	/	From 19 to 36	[13,15]
Pulsed DC sputtering	1.3	200	$Ar + N_2$	250.E3	From 20 to 35	[16]

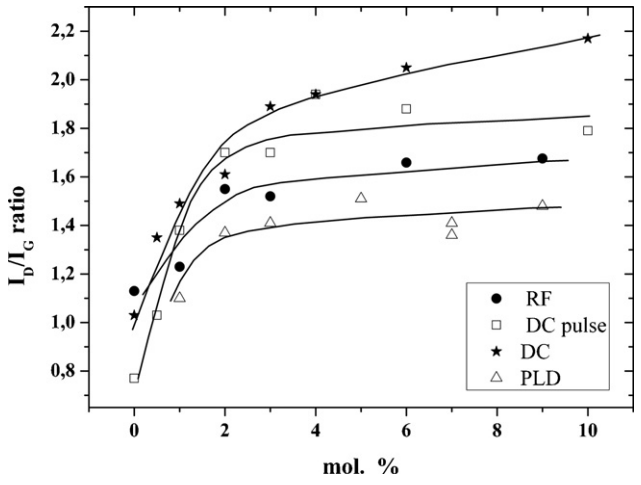

Fig. 2. Variation of the I_D/I_G ratio versus the $N_2/Ar + N_2$ ratio (i.e. mol.%). The line is only a guide for the eyes.

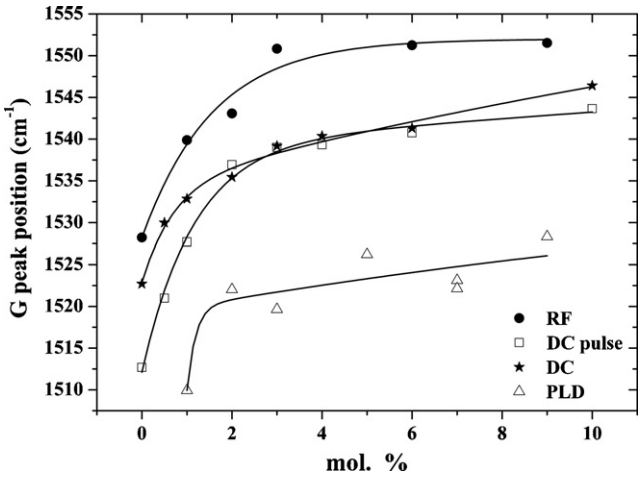

Fig. 3. Variation of the G peak position versus the $N_2/Ar + N_2$ ratio (i.e. mol.%). The line is only a guide for the eyes.

More supporting evidence for the above argument of bonding structure changes in these samples can be supplied from the correlation between the optical gap and the Raman features.

The optical gap E_g of amorphous semiconductors is conventionally is obtained through the Tauc plot [18] written as:

$$\alpha E = B(E - E_g)^2 \quad (1)$$

where B is a constant proportional to the square of the density of states and α is the absorption of the films, obtained from the transmittance, T, of the films:

$$\alpha = -\frac{(\ln T)}{d} \qquad d : \text{film thickness} \quad (2)$$

The intercept of the Tauc's slope in the phonon energy axis gives the optical band gap.

We report in Fig. 4, the variation of the obtained optical gaps versus the $N_2/Ar + N_2$ ratio for different series of samples. For the DC samples, E_g is seen to decrease from 0.9 to 0.4 eV with increasing the percentage of nitrogen gas in the mixture from 0 to 3%. The gap value falled down from 1.1 to 0.5 eV for the DC pulsed samples. Finally for DC the RF sputtering samples, E_g remained nearly constant for the higher $N_2/Ar + N_2$ ratio values up to 10%, while the E_g values for the DC pulsed samples were increase slowly in the range of the studied $N_2/Ar + N_2$ ratio. The analysis of these

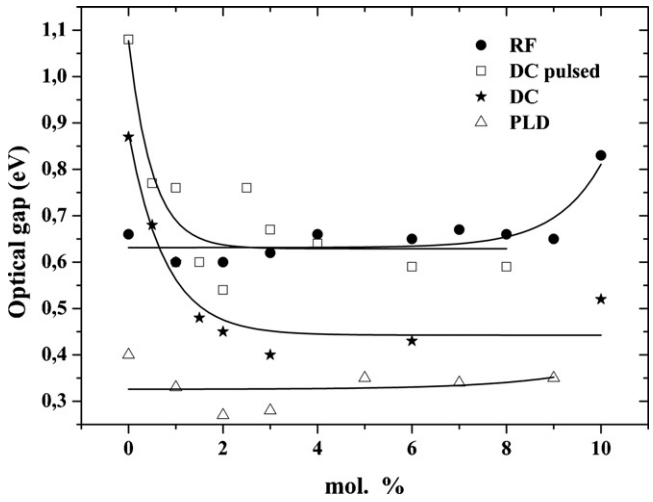

Fig. 4. Variation of the optical gap versus the $N_2/Ar + N_2$ ratio (i.e. mol.%). The line is only a guide for the eyes.

collections of gaps is difficult and reveals that direct correlation with the sp^2 fraction or the $N_2/Ar + N_2$ ratio and depends on the mechanisms of growth of the studied films.

Further information about the film microstructure was obtained by the electrical measurements, which is sensitive to the microstructure of the deposited films. As shown in Fig. 5, the conductivity measurements presented an antagonist variation in comparison to the gap ones. In the first stage of the $N_2/Ar + N_2$ ratio (from 0 to 2–3%), the conductivity increased for all the techniques. The more important increments of the conductivity were seen for the DC pulsed samples with a variation over 4 decades (from 10^{-6} to 10^{-2} S cm^{-1}) whereas, for the DC and the RF samples, the conductivity increased from 10^{-4} to 0.1 S cm^{-1} and from 0.01 to 0.1, respectively with increasing the N_2 content into plasma from 0 to 2–3%. For the higher N content into plasma (up to 10%), the conductivity remained constant for the DC and DC pulsed samples but decreased from 0.1 to 10^{-4} S cm^{-1} for the RF sputtering samples.

4. Discussion

A global overview of the physical characteristics for all series of samples allows us to divide the behaviour into two different regimes: "the low N content", corresponding to the percentage of nitrogen gas in the mixture for the sputtering techniques below 3% and "the high N content" for the value above 3%. In this way let us consider the low N content region for the sputtering techniques first.

4.1. Low N content region

The simultaneous increase in the G peak position and the I_D/I_G ratio versus the $N_2/Ar + N_2$ ratio suggest both an enhanced sp^2 fraction (the π states) and the disorder in the film [19,22]. The G peak behaviour is characteristic of a transition to more graphitic films, while the I_D/I_G ratio evolution causes the sp^2 clusters to become larger and can be is associated to the disorder due to the incoming species bombardment, for pulsed DC samples, and to the incorporation of nitrogen in the films (DC and RF samples), which breaks the long-range order of the graphitic structure [5,18]. This result can well describe the evolution of E_g reported in Fig. 4. Indeed, it was reported that the decrease of E_g with nitrogen incorporation is related to the increase in the size of the sp^2 clusters (the π states) [5,18]. Because the bonding in a-CN_x films consists of noninteracting π and σ bonds in a similar way as in a-C

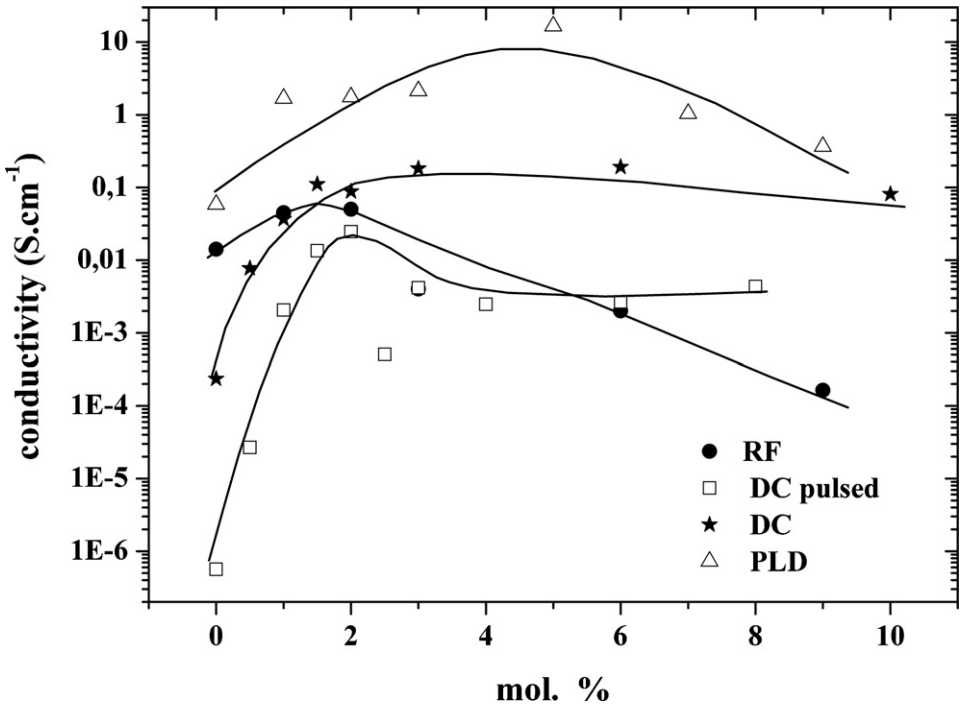

Fig. 5. Variation of the conductivity versus the $N_2/Ar + N_2$ ratio (i.e. mol.%). The line is only a guide for the eyes.

films, the electronic and optical properties should also be controlled by the π bonding that lies closest to the Fermi Level [5–10]. According to Robertson, the optical gap is attributed to the transitions between weakly localised states of the π–π* states that come from the sp^2 configurations atoms in the network. These sp^2 sites tend to pair up, forming large clusters embedded in a mainly sp^3 matrix. The clustering model of the sp^2 sites have to be taken with certain precautions since the disorder associated with the energetic bombardment during the deposition inhibits ring clustering and distorts the planar configuration of C sp^2 atoms, thus affecting the optical properties [23,24].

The gap values for all series of samples allow us to consider that the studied a-CN_x films are highly sp^2. The behaviour of E_g observed in Fig. 4 can be connected to the enhancement of the amount of the sp^2 bonds in the global network in good agreement with the Raman results reported above. This increase of sp^2 sites can be well described by the notion of clusters (involving a coordination of the π states over a typical dimension which corresponds to the cluster size). The dimension of the cluster is known to be the main factor that determines the gap value, i.e. an increase of the cluster size induces a reduction of gap value [23]. Summarising, we can conclude that the increase in I_D/I_G and the decrease in optical gap signifies the optical gap lowering as a result of an enhanced sp^2 fraction in the film induced by nitrogen incorporation in the a-C network.

Notice that the gap variations are more important for the DC and DC pulsed samples than for the RF ones. This difference suggested that the N incorporation into the DC and DC pulsed samples inducted a clear increase of cluster size, whereas in the RF samples, the increase of size might be balanced by an increase of the disorder explaining the low variation of the gap. Similarly, the higher value of the G peak position for the RF samples compared to DC and pulsed DC ones suggested that this value can be due to a larger quantity of clusters.

More supporting evidence for the above arguments about the bonding structure variations in these samples can be supplied from the conductivity measurements. Indeed, the electrical properties of amorphous carbon have been proposed to be dominated by the π states of the sp^2 sites because they form the valence and conduction band edges [23,24]. It was reported that the conduction mechanisms in amorphous semiconductor are governed by two processes; thermally activated process (described in the $R(T)$ measurements by a Arrhénius plot) and variable range hopping (VRH) conduction (described by a $1/T^{1/4}$ law) [26–28,24,29,30]. The main difference of these two types of conduction mechanisms comes from the type of localisation of the electronic carriers involved in the conduction. Thus, highly localised states located within the mobility gap (near the Fermi level or/and in the band tail states) are the origin of VRH conduction while weakly localised states control the thermally activated conduction. The correlation between the optical gap, the cluster size and the conductivity results for the DC and DC pulsed samples could be explained by an increase of the weakly localised states, assuming that an increase of cluster size favours the thermally activated conduction (increasing the "delocalisation" of the π states over the cluster) whereas an increase of number of cluster act in favour of VRH conduction (an increase of cluster's number increase the hopping sites into the network). Beyond the same trends, the lower variation of conductivity for the RF samples add to the low variation of gap (i.e. low increase of cluster size) and increase of G peak position (i.e. increase of the sp^2 configuration) suggest that the N incorporation into the carbon films favour the highly localised π states rather than the weakly localised ones. Further investigation of the conductivity versus temperature will allow us to give more reliability to this argument.

4.2. High N content region

The high N content region is characterised by the slight variation of the optical gap, the electrical conductivity and the Raman features (nearly constant behaviour) for all the techniques. The saturation in the film properties as the $N_2/Ar + N_2$ ratio

increased might be explained by the microstructure changes due to the N incorporation within the films.

As reported above, the gradual change in the band gap versus the $N_2/Ar + N_2$ ratio seems to be related primarily to the width of the π bands, which depends on the cluster size such that the optical gap decreases inversely with cluster size. Nevertheless, the optical responses of the films at high N content do not only work for the assumption of cluster size, but also with the degree of disorder associated with the growth conditions. The incorporation of nitrogen breaks the long-range order of the graphitic structure and promotes both the clustering of Csp^2 sites and the disorder in theses ring structures. Indeed, when N is introduced into a carbon network, the CN vibration frequencies for chain-like molecules and ring-like molecules are very close to those of pure carbon. The modes are delocalised over both C and N sites due to the capability of N to acquire the same hybridisations as C atoms. In addition, with increasing the nitrogen content most of the network becomes terminated by NH or $CNsp^1$ (i.e. (C≡N)) bonds, which may terminate a chain or form part of network within film the structure of the films and determines the extent of the void structure limiting the cluster size increase [5,25–28]. The films grown under low ion bombardment (i.e. DC and RF samples) exhibit a high concentration of C≡N group [5,25–28]. For pulsed DC samples, the formation of the clusters is opposed by the disorder, due to ion bombardment, which could oppose ring clustering and distorts the local planar configuration of Csp^2 atoms [5,22]. So, our results suggest that beside the transition to Csp^2, the disorder of the C–C network is enhanced with increasing $N_2/Ar + N_2$ as suggested by the I_D/I_G ratio (Fig. 2) which, exhibits a similar tendency and suggests the increase both in the graphite size and number of the graphitic Csp^2 clusters: the translation periodicity of the atomic network of the solid is disturbed by bond-angle distortions and particle size effects caused by the nitrogen incorporation on the carbon structure. This nanoclustering of the Csp^2 sites influences mainly the optical responses of the films. Thus, the evolution of the gap can be analysed in terms of both cluster size and the local distortion of the π bonding [5,22].

The decrease of conductivity added to the observation of the constant behaviour of the Raman parameters for the RF samples suggest that the N incorporation into the network produce significant changes in the bonding characteristics; i.e. an increase of disorder into the sp^2 clusters and a loss of connectivity between them [26–28,24]. N terminal bonding (C–N triple bond or N substitution into aromatic ring [5,19] have been observed and have to be confirmed by other characterisations techniques.

The low variations in the high N content region and the maximum value, for all the techniques, of both the gap and the conductivity at the boarder between the two regions suggest two mains arguments: in the one hand, the N incorporation favour the formation of a maximum cluster size and further addition of nitrogen into the network can not increase them anymore, in the other hand, the N incorporation into the network is efficient in the low values of the $N_2/Ar + N_2$ ratio and the N content (in term of at.% into the network) saturate above this maximum value.

5. Conclusion

The correlation between the microstructure and the optoelectronical properties of a-CN_x films, deposited by three different deposition techniques, with different nitrogen contents were investigated using Raman spectroscopy, optical transmission and electrical conductivity experiments. The results of Raman spectroscopy suggest an increase in the fraction of Csp^2 coordinated carbon in the film with the $N_2/Ar + N_2$ ratio but with a still very high disorder form of Csp^2. The decrease of the optical gap as function N content has been discussed in terms of the Csp^2 sites fraction and arrangement within the films. So, beside the sp^2 content, the distribution and local bonding of sp^2 bond play a significant role in the electronic properties of the a-CN_x films. The low N content samples deposited by soft deposition technique (DC and RF sputtering) seem to be an interesting material to produce films with interest properties for optoelectronic applications considering the facility to control the gas composition as a key parameter. The comparison between the three deposition techniques gives us interesting perspective to understand the N incorporation mechanisms into the amorphous carbon network.

References

[1] A.Y. Liu, M.L. Cohen, Science 245 (1989) 841.
[2] L. Hultman, J. Neidhardt, N. Hellgren, H. Sjöström, J.-E. Sundgren, Mater. Res. Soc. Bull. (2003) 194.
[3] M. Neuhaeuser, H. Hilgers, P. Joeris, R. White, J. Wideln, Diamond Relat. Mater. 9 (2000) 1500.
[4] C. Ronning, U. Griesmeier, M. Gross, H.C. Hofsäass, R.G. Downing, G.P. Lamaze, Diamond Relat. Mater. 4 (1995) 666.
[5] M. Lejeune, O. Durand-Drouhin, S. Charvet, A. Grosman, C. Ortega, M. Benlahsen, Thin Sol. Films 444 (2003) 1.
[6] S.R.P. Silva, B. Rafferty, G.A.J. Amaratunga, J. Schawn, D.F. Franceschini, L.M. Brown, Diamond Relat. Mater. 5 (1996) 401.
[7] M. Rusop, T. Soga, T. Jimbo, Diamond Relat. Mater. 13 (2004) 2187.
[8] R.C. Smith, J.D. Carey, C.H.P. Poa, D.C. Cox, S.R.P. Silva, J. Appl. Phys. 95 (2004) 3153.
[9] S.R.P. Silva, J.D. Carey, X. Guo, W.M. Tsang, C.H.P. Poa, Thin Sol. Films 79 (2005) 482.
[10] J.D. Carey, R.C. Smith, S.R.P. Silva, J. Mat. Sci.––Mat. Electron. 17 (2006) 405.
[11] R. Kalfoten, T. Sebald, G. Weise, Thin Sol. Films 290 (1996) 112.
[12] M. Benlahsen, M. Therasse, Carbon 42 (1) (2004) 225.
[13] B.K. De Koven, P.R. Ward, R.E. Weiss, D.J. Christie, R.A. Scholl, F. Tomasel, A. Anders, 46th Annual Technical Proceedings, 2003, p. 158.
[14] X.B. Tian, D.T.K. Kwok, P.K. Chu, J. Appl. Phys. 88 (2000) 4961.
[15] S.E. Rodil, S. Muhl, S. Maca, A.C. Ferrari, Thin Sol. Films 433 (1–2) (2003) 119.
[16] T. Moiseev, D.C. Cameron, Surf. Coat. Technol. 200 (18–19) (2006) 5306.
[17] N.F. Mott, E.A. Davis, Electronic Processes in Non-Crystalline Materials, second ed., Oxford University Press, 1979.
[18] A.C. Ferrari, S.E. Rodil, J. Robertson, Phys. Rev. B 67 (2003) 1553061.
[19] M.A. Tamor, W.C. Vassell, J. Appl. Phys. 76 (1994) 3823.
[20] F. Tuinstra, J.L. Koenig, J. Chem. Phys. 53 (1970) 1126.
[21] A.C. Ferrari, J. Robertson, Phys. Rev. B 61 (2000) 14095.
[22] (a) J. Robertson, E.P. O'Reilly, Phys. Rev. B 35 (1987) 2946;
(b) J. Robertson, Diamond Relat. Mater. 4 (1995) 297.
[23] C. Oppedisano, A. Tagliaferro, Appl. Phys. Lett. 75 (1999) 3650.
[24] E.A. Davis, N.F. Mott, Philos. Mag. 22 (1970) 903.
[25] G. Abrasonis, R. Gago, M. Vinnichenko, U. Kreissig, A. Kolitsch, W. Möller, Phys. Rev. B 73 (2006) 125427.
[26] M.A. Monclus, D.C. Cameron, A.K.M.S. Chowdhurry, Thin Sol. Films 341 (1999) 94.
[27] C. Godet, N.M.J. Conway, J.E. Bourée, K. Bouamra, A. Grosman, C. Ortega, J. Appl. Phys. 91 (2002) 4154.
[28] N.E. Derradji, M.L. Mahdjoubi, H. Belkhir, N. Mumumbila, B. Angleraud, P.Y. Tessier, Thin Sol. Films 482 (2005) 258.
[29] E. Broitman, N. Hellgren, K. Järrendahl, J. Appl. Phys. 89 (2) (2001) 1184.
[30] M.A. Monclus, D.C. Cameron, R. Barklie, M. Collins, Surf. Coat. Technol. 116–119 (1999) 54.